200
$8-6-80$

$\mathcal{D}ri\,16ff_l$

orln

OAK
RIDGE
NATIONAL
LABORATORY

UNION
CARBIDE

MASTER

The Interaction of Silver and Palladium with Silicon Carbide in HTGR Fuel Particles— Preliminary Report

R. J. Lauf

DISCLAIMER

This report was prepared as an account of work sponsored by an agency of the United States Government. Neither the United States Government nor any agency Thereof, nor any of their employees, makes any warranty, express or implied, or assumes any legal liability or responsibility for the accuracy, completeness, or usefulness of any information, apparatus, product, or process disclosed, or represents that its use would not infringe privately owned rights. Reference herein to any specific commercial product, process, or service by trade name, trademark, manufacturer, or otherwise does not necessarily constitute or imply its endorsement, recommendation, or favoring by the United States Government or any agency thereof. The views and opinions of authors expressed herein do not necessarily state or reflect those of the United States Government or any agency thereof.

ORNL/TM-7393
Distribution
Category UC-77

Contract No. W-7405-eng-26

METALS AND CERAMICS DIVISION

HTGR BASE TECHNOLOGY PROGRAM

Fueled Graphite Development (189a 01330)

THE INTERACTION OF SILVER AND PALLADIUM WITH SILICON CARBIDE
IN HTGR FUEL PARTICLES — PRELIMINARY REPORT

R. J. Lauf

Date Published: July 1980

NOTICE: This document contains information of a
preliminary nature. It is subject to revision
or correction and therefore does not represent a
final report.

OAK RIDGE NATIONAL LABORATORY
Oak Ridge, Tennessee 37830
operated by
UNION CARBIDE CORPORATION
for the
DEPARTMENT OF ENERGY

CONTENTS

THE INTERACTION OF SILVER AND PALLADIUM WITH SILICON CARBIDE
IN HTGR FUEL PARTICLES — PRELIMINARY REPORT

R. J. Lauf

ABSTRACT

Fuel particles for the High-Temperature Gas-Cooled
Reactor contained a layer of pyrolytic silicon carbide, which
acts as a pressure vessel and provides containment for
metallic fission products. The SiC layer is deposited by the
thermal decomposition of methyltrichlorosilane (CH_3SiCl_3 or
MTS) in an excess of hydrogen. Certain fission products,
notably silver and palladium, can cause degradation of the SiC
during irradiation. The purpose of this study is to develop a
quantitative data base to better understand noble-metal attack
as well as to evaluate the relationship between SiC deposition
conditions and noble-metal release.

The interaction between SiC and noble-metal fission pro-
duct elements was investigated in the temperature range 1200·
to 1500°C. Simulated high-burnup Triso-coated fuel particles
were fabricated by impregnating UO_2 microspheres with metallic
Ag or Pd followed by coating them under systematically varied
conditions. The coated particles were mounted in carbon
disks and were annealed for 2000 h in a thermal gradient of
27.5°C/mm.

Metallographic examination revealed three modes of
interaction: local attack of the SiC associated with nodules
of Ag or Pd, presence of free metal particles partway through
the coating thickness where no visible penetration path
existed, and accumulation of free metal along circumferential
striations in coatings deposited at or below 1550°C.

The rates of attack of SiC by Ag and Pd are strongly
temperature dependent. The Pd attack rate increased slightly
with increasing SiC coating rate, while SiC deposition tem-
perature has little effect. Since the Pd attack rates during
out-of-reactor annealing agree with rates measured in irra-
diated particles, it is likely that attack is controlled by
grain boundary diffusion.

INTRODUCTION

Fuel microspheres for the High-Temperature Gas-Cooled Reactor (HTGR)
are coated with several layers of pyrolytic carbon (PyC) and a layer of
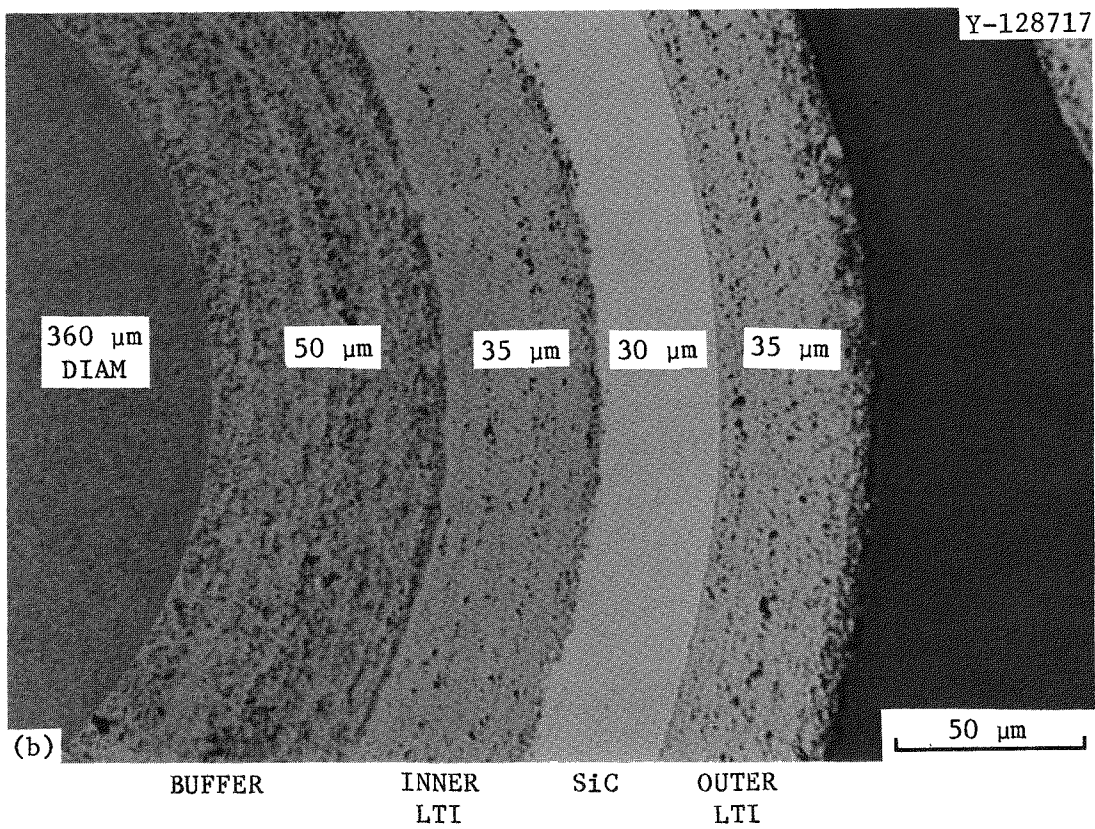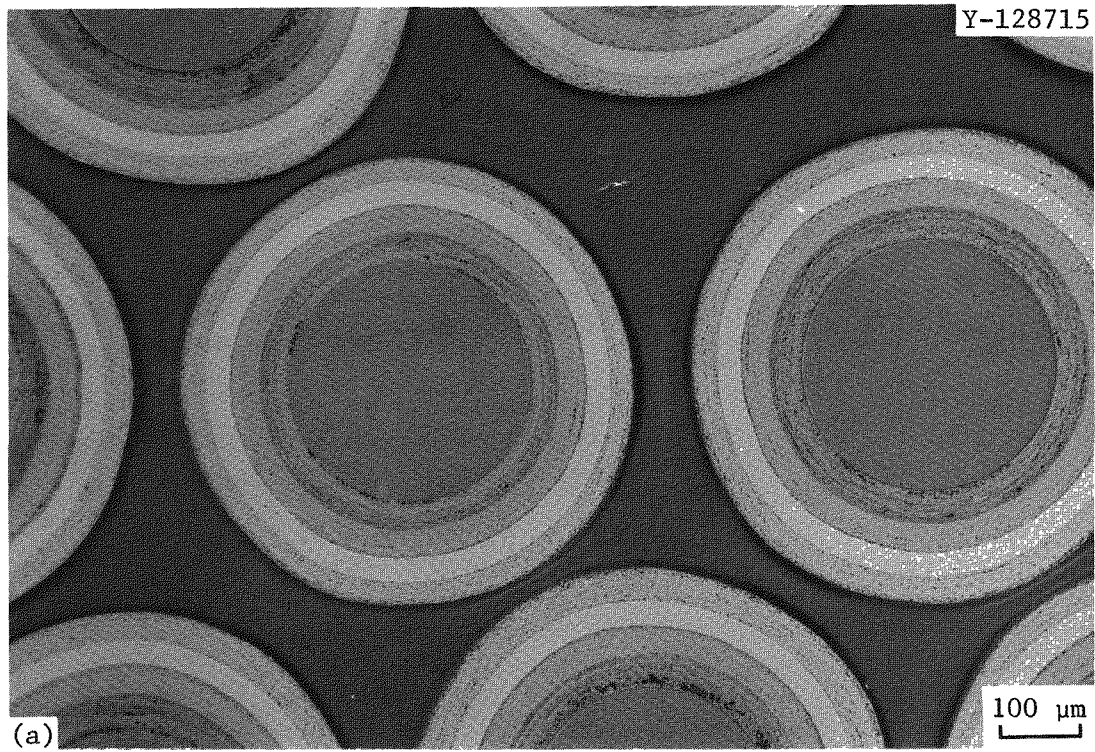silicon carbide, as shown in Fig. 1. The low-density buffer PyC layer

Fig. 1. Triso-Coated HTGR Fuel Particles.

provides void volume for fission gas retention. The inner low-temperature isotropic (LTI) PyC layer provides mechanical strength to resist stresses generated by the fission gas pressure (typically several hundred times atmospheric pressure). The inner LTI layer also provides the containment for certain fission products that are produced in the kernel and that diffuse readily through the buffer layer. The SiC layer serves as a structural member (the complete fuel particle becomes a miniature pressure vessel) and is the primary containment for several fission products, namely, strontium, cesium, barium, and certain rare earths. These elements are the dominant solid products from the fission of ^{235}U under standard conditions. The outer LTI PyC coating protects the SiC from mechanical damage during fabrication of the particles into carbon fuel rods.

It has been established that a SiC layer of nearly theoretical density provides adequate containment of fission products during irradiation of high-enriched uranium (HEU)* fuels.[1] While low-enriched uranium (LEU)* and medium-enriched uranium (MEU)* fuels are feasible from a neutronic standpoint, the greater amount of ^{238}U causes a shift in fission yields toward the yield spectrum of ^{239}Pu. The most important consequence of this is the increased yield of noble metals, especially silver and palladium. These elements are particularly agressive toward SiC at HTGR operating temperatures. Thus, a major goal of the present SiC development program is the optimization of the SiC coating for noble-metal retention.

To clarify the relationships between the deposition conditions and the coating microstructures and between the coating microstructures and noble-metal retention, 12 SiC coatings were deposited under systematically varied conditions of temperature and coating rate. For each SiC coating type, Biso-coated† kernels of UO_2, UO_2 plus Ag, and UO_2 plus Pd were included. The different coating types (taken primarily from the pure UO_2 kernels) were characterized by several techniques. The dependence of SiC coating microstructure and properties on deposition conditions was the

---

*Nominal enrichments are HEU, 93% ^{235}U; MEU, 20 to 40% ^{235}U; and LEU, less than 10% ^{235}U.

†That is, kernels coated with the buffer and inner LTI pyrocarbon layers.

subject of a previous report[2] and is under continuing study. The present
report describes the results of annealing each of the coated particle
types in a thermal gradient to simulate conditions in an operating HTGR.
The objective is to determine whether some SiC coatings are more resistant
to noble-metal release than others deposited under slightly different
conditions.

EXPERIMENTAL MATERIALS AND PROCEDURES

Fabrication of Simulated Fuel Microspheres

The first requirement of studying the interactions between SiC
coatings and selected fission products without the difficulties associated
with examining irradiated fuel was fabricating two batches of UO_2 micro-
spheres doped with Ag and Pd, respectively. Ideally, such experimental
particles should be comparable in size to standard fuel microspheres and
should contain a fine distribution of fission product. Furthermore, the
particles must be reasonably spherical so that standard fluidized-bed
coating practice can be used. Finally, it must be possible to Biso-coat
the particles without volatilizing the fission product. Fabricating
microspheres that fulfilled these requirements was a major experimental
task.

Three batches of calcined uranium oxide microspheres produced by the
chemical gelation process were obtained before sintering. One batch was
sintered in the usual manner and was Biso-coated without the addition of
any fission product elements. These particles, after coating with SiC,
were annealed alongside those containing fission product elements to allow
the study of microstructural changes resulting from thermal gradient
annealing alone.

The second batch was sintered to about 60% of theoretical density by
heating to 700°C in flowing hydrogen and then to 1200°C in argon. After
cooling, the particles were infiltrated with aqueous silver nitrate
solution, were rinsed, and were dried overnight at about 110°C in air.
Some metallic Ag was visible on the particle surfaces at this stage. To
fully reduce the Ag and remove any remaining NO_3^-, the particles were

heated to 600°C in flowing hydrogen and held for 1 h. To Biso-coat these particles the standard procedure* was modified. Before depositing the buffer coating, a thin carbon layer was deposited at about 800°C. This prevented the Ag from boiling off when the buffer and inner LTI layers were deposited. The fine distribution of Ag within the Biso-coated kernel is shown optically in Fig. 2(a) and by electron microprobe analysis in Fig. 3.

The third batch was sintered to about 30% of theoretical density by heating to 700°C in flowing hydrogen followed by heating to 1000°C in flowing argon. The particles were infiltrated with aqueous $PdCl_2$, then rinsed and dried as before. The dried spheres were heated to 600°C in flowing hydrogen, were held for 1 h, and then were heated to 1400°C in argon for final sintering. (This sequence was possible because of the higher melting point of Pd.) Some of the particles developed a rough sur-face during sintering, but this did not affect the subsequent coating steps. Figure 2(b) shows a Pd-doped kernel, in which the Pd appears as extremely small round specks. An electron microprobe display of the Pd distribution is presented in Fig. 4.

The pertinent data for all three batches of kernels after Biso-coating are given in Table 1.

---

*Process procedure MET-CER-PP-12.

Table 1. Properties of UO_2 Microspheres for Coating Experiments

Kernel Type	Fission Product Concentration (wt %)	Burnup (% FIMA[a])	Diameter,[b] μm		Thickness,[b] μm	
			Kernel	Total	Buffer	Inner LTI
UO_2	0	0	411(45)	497(33)	46(8)	40(4)
UO_2 + Ag	1.26	~200[c]	380(40)	542(20)	45(5)	45(5)
UO_2 + Pd	0.54	~10	360(50)	523(35)	45(6)	38(4)

[a]FIMA = fissions per initial metal atom.

[b]Numbers in parentheses are ± deviations.

[c]The Ag-doped kernels contained substantially more Ag than would a fuel particle at end of life. This occurred because it was impossible to accurately predict the efficiency of the infiltration-reduction process.

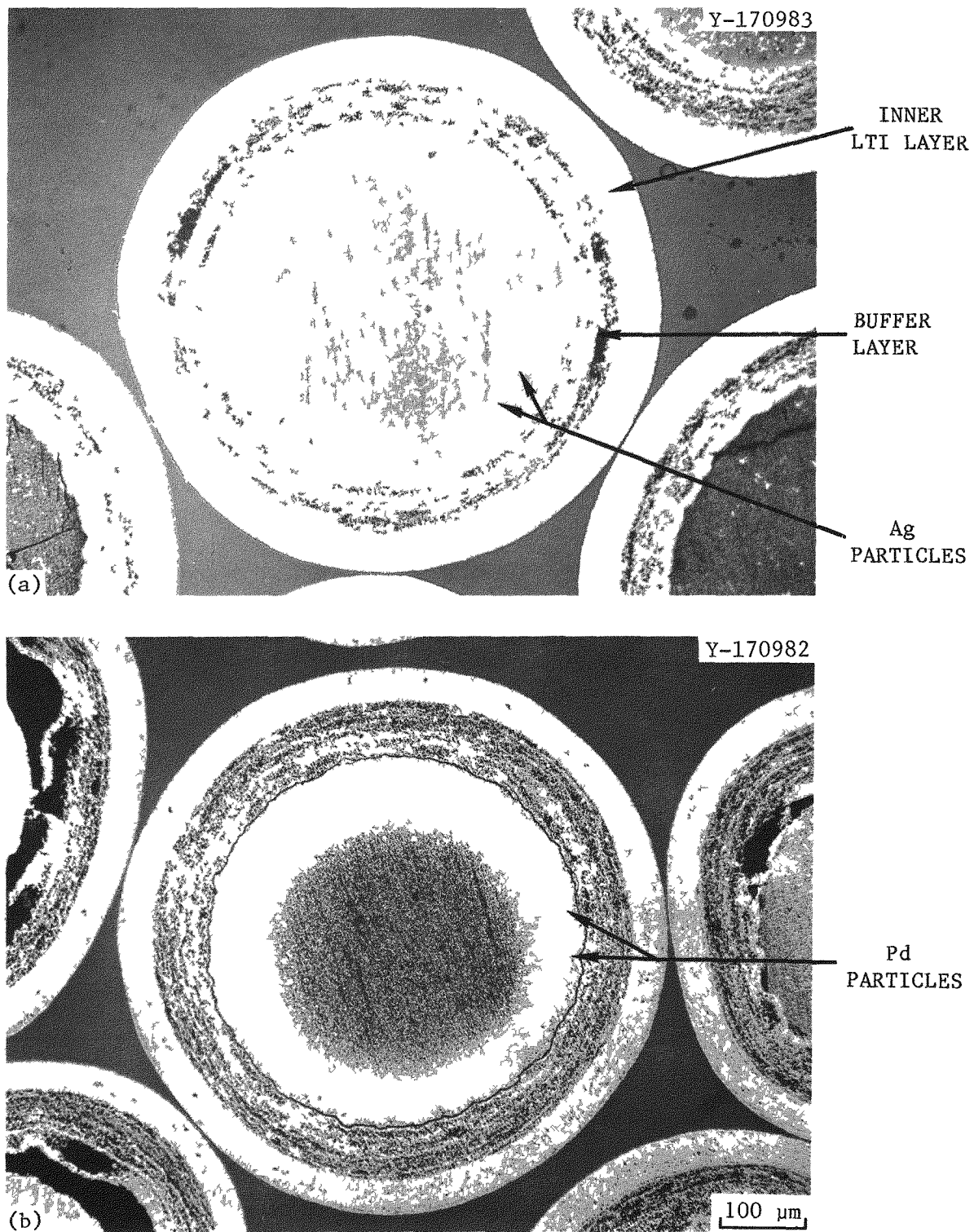Fig. 2. Optical Micrographs of Biso-Coated UO₂ Microspheres Doped with Fission Product Elements. (a) UO₂ plus Ag. (b) UO₂ plus Pd.
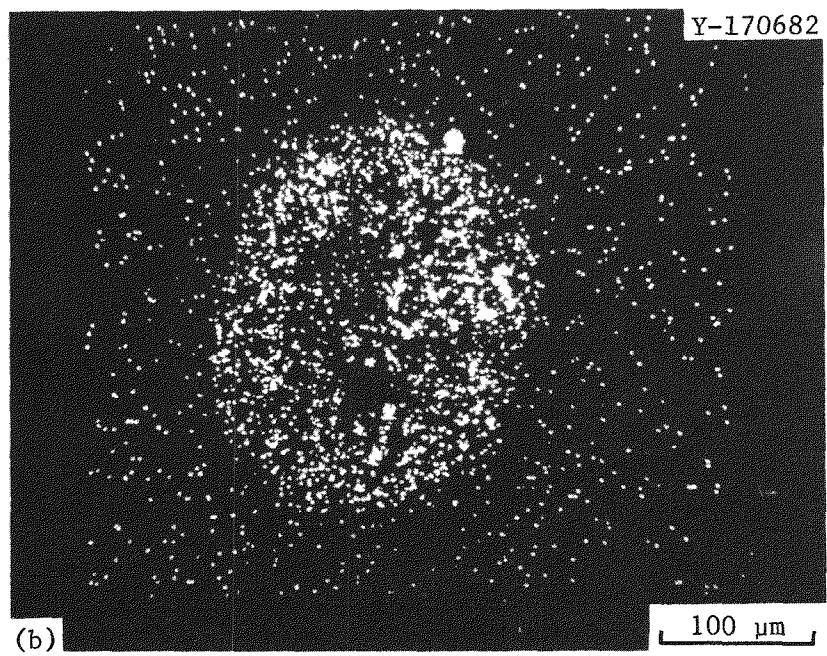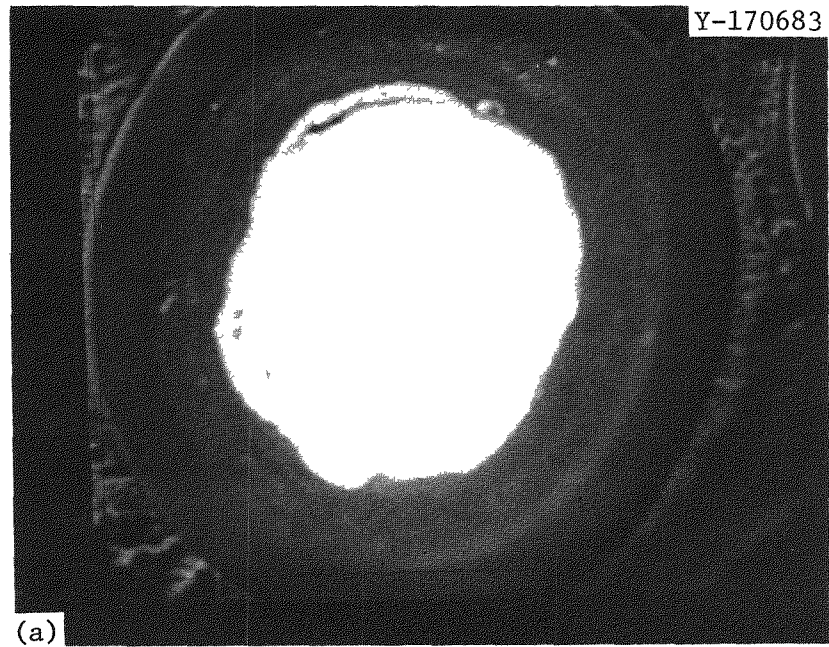
Fig. 3. Electron Microprobe Displays of Biso-Coated UO_2 Microspheres Doped with Ag. (a) Backscattered electron image. (b) Ag $L\alpha$ image.
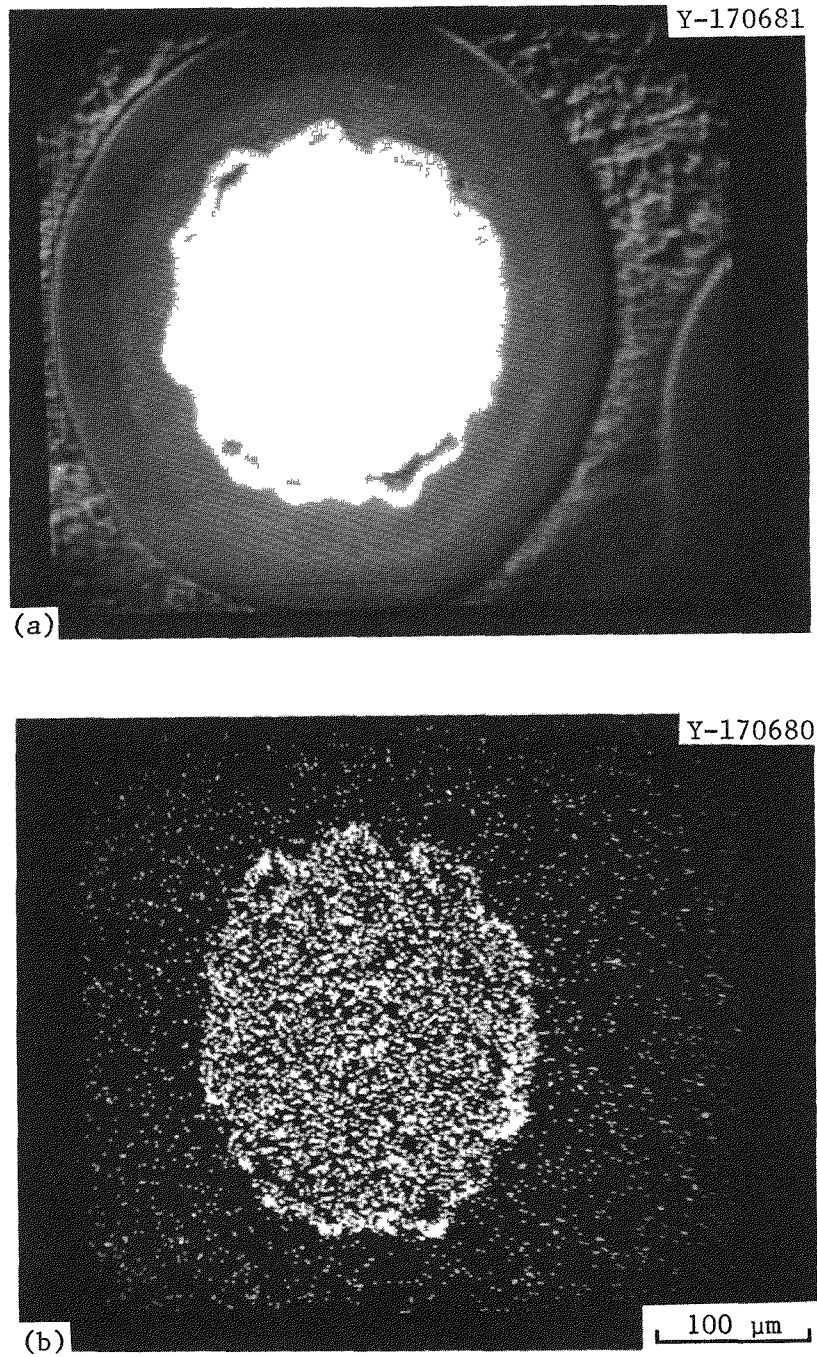
Fig. 4. Electron Microprobe Displays of Biso-Coated UO_2 Microspheres Doped with Pd. (a) Backscattered electron image. (b) Pd $L\alpha$ image.

Deposition of SiC Coatings

Coatings were deposited by thermal decomposition of methyltrichloro-
silane (CH_3SiCl_3 or MTS) in an excess of hydrogen. Details of the coating
apparatus and procedure are given elsewhere.[3] In the present study we
investigated 12 sets of coating conditions. For each set the three dif-
ferent kernel types were coated separately. Thus, a total of 36 coating
runs were made. Table 2 summarizes the data for all coating runs used in
this study.

We assumed that coatings deposited on all types of kernels under
nearly identical conditions would have similar structure and properties.
To verify this, coating samples were removed from several batches that
contained Ag or Pd, and their densities were compared with those of
coatings deposited on UO_2 kernels under corresponding conditions. As
Table 2 shows, the initial assumption was verified by the results of den-
sity measurements.

Annealing Tests

To simulate thermal conditions in an HTGR, the experimental particles
were annealed in a thermal gradient furnace. The apparatus and technique
are described in detail by Lindemer and Pearson[4] and may be briefly sum-
marized as follows. Approximately 20 particles from each of the 36
coating batches were mounted in carbon disks. After the disks were cured
and heat-treated, they were cemented into graphite plates, which held them
in the gradient furnace. Since each plate had provision for 3 disks, 12
plates were used, 1 for each set of coating conditions. Each plate thus
contained samples of the three types of particles (UO_2, UO_2 plus Ag, and
UO_2 plus Pd), all coated under the same conditions. The sample holder is
illustrated in Fig. 5.

The operating conditions of the gradient furnace were set to provide
a thermal gradient of about 27.5°C/mm across the diameter of each disk.
The hot side was held at 1500°C, and since the particles were spread over
a distance of about 10 mm, individual particle temperatures ranged from

Table 2. Summary of Experimental SiC Coating Runs

Batch[a]	Run	Deposition Temperature (°C)	Coating Rate (μm/min)	SiC Density Mg/m^3
D-1	SC-483	1500	0.42	3.208
D-2	484	1550	0.40	3.212
D-3	485	1650	0.43	3.218
D-4	487	1700	0.42	3.197
D-5	472	1500	0.70	3.190
D-6	476	1550	0.75	3.207
D-7	477	1650	0.71	3.203
D-8	475	1700	0.50	3.195
D-9	479	1500	1.20	3.156
D-10	473	1550	1.01	3.195
D-11	480	1650	0.95	3.207
D-12	481	1700	1.06	3.206
Ag-1	508	1500	0.40	
Ag-2	511	1550	0.39	
Ag-3	521	1650	0.32	
Ag-4	518	1700	0.37	
Ag-5	509	1500	0.70	
Ag-6	505	1550	0.64	3.207
Ag-7	519	1650	0.73	
Ag-8	507	1700	0.63	
Ag-9	510	1500	1.24	
Ag-10	512	1550	1.19	
Ag-11	513	1650	0.91	
Ag-12	514	1700	1.16	
Pd-1	499	1500	0.44	3.208
Pd-2	500	1550	0.39	
Pd-3	522	1650	0.40	
Pd-4	502	1700	0.33	
Pd-5	488	1500	0.79	
Pd-6	489	1550	0.78	
Pd-7	492	1650	0.50	
Pd-8	493	1700	0.79	
Pd-9	494	1500	1.04	3.184
Pd-10	498	1550	1.03	
Pd-11	496	1650	0.97	3.207
Pd-12	497	1700	1.29	

[a]Batch designations are as follows: D = UO_2 kernels, Ag = UO_2 + Ag kernels, and Pd = UO_2 + Pd kernels.

ORNL DWG 75-14996

HEATING
ELEMENT

GRAPHITE SUPPORT

GRAPHITE FELT
INSULATION

GRAPHITE DISC
HOLDER

OPTICAL
PYROMETER
SIGHT HOLES

"A"

SAMPLE
DISCS

"A"

SECTION "A-A"

GRAPHITE DISC HOLDER
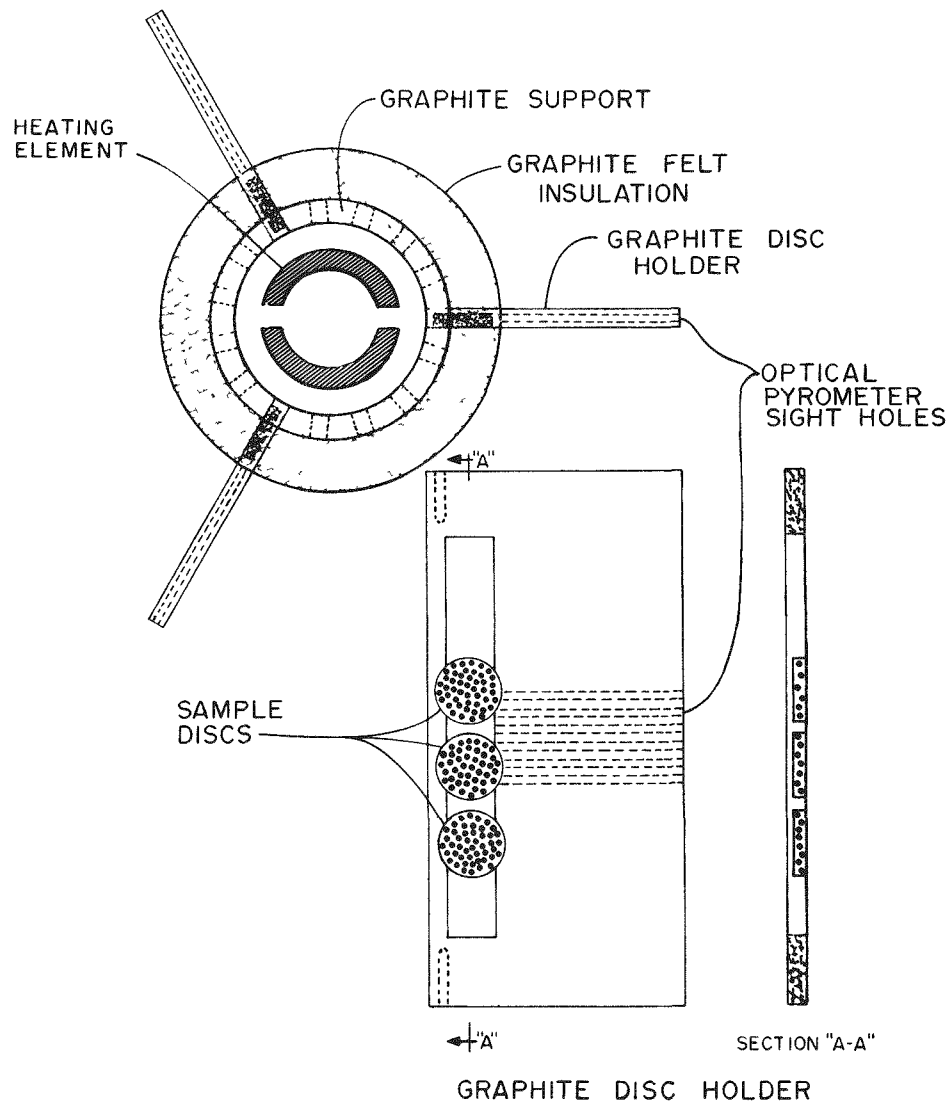
Fig. 5. Graphite Holder Used to Support Experimental Particles for Annealing in Thermal Gradient Furnace.

about 1500 to about 1225°C. Exact positions relative to the hot face were measured on radiographs of the completed assemblies. The exact temperature of each particle could thus be calculated subsequently.

The plates were removed from the furnace and radiographed after 400 and 1024 h of annealing to monitor any changes such as kernel migration or gross coating attack. After a total of 2000 h of annealing, the disks were removed and prepared for metallographic examination.

RESULTS AND DISCUSSION

Urania Kernels

The coated particles that did not contain fission product elements showed no SiC degradation after 2000 h of annealing in the thermal gradient furnace. Some kernels, particularly those at 1450 to 1500°C, exhibited slight shrinkage. This evidently resulted from further sintering during the anneal. Even in these cases the SiC and PyC layers were unaffected.

Urania Kernels Containing Palladium

The coated particles containing Pd showed several effects:

1. Local spots were attacked in all batches, particularly on the cold sides of the particles. The attack was characterized by partial penetration of the SiC layer, generally associated with a buildup of Pd at the SiC-inner LTI interface. Free Pd and possibly an unidentified reaction product usually formed a nodule at the attack site, and the area was nearly always optically anisotropic. The overall appearance of the reaction zone, shown in Fig. 6, is identical to that of similar attack seen in irradiated microspheres.[5]

2. Small bright specks that appear to be Pd occurred at some distance into the coating thickness in some specimens where no localized attack could be seen. We do not know whether these are accumulations following solid-state diffusion or protuberances on the surface of an attack nodule that is too far below or above the plane of polish to be visible.

3. Metallic spots (probably Pd) distributed along circumferential striations in the SiC were seen in coatings deposited at 1500°C. A typical view of this phenomenon is shown in Fig. 7.

We attempted to quantify the Pd attack for comparison with irradiation results. Each disk was examined optically, and particles were selected that had visible nodules of attack. The nodules were photographed at 1000×, and each particle was located on the appropriate
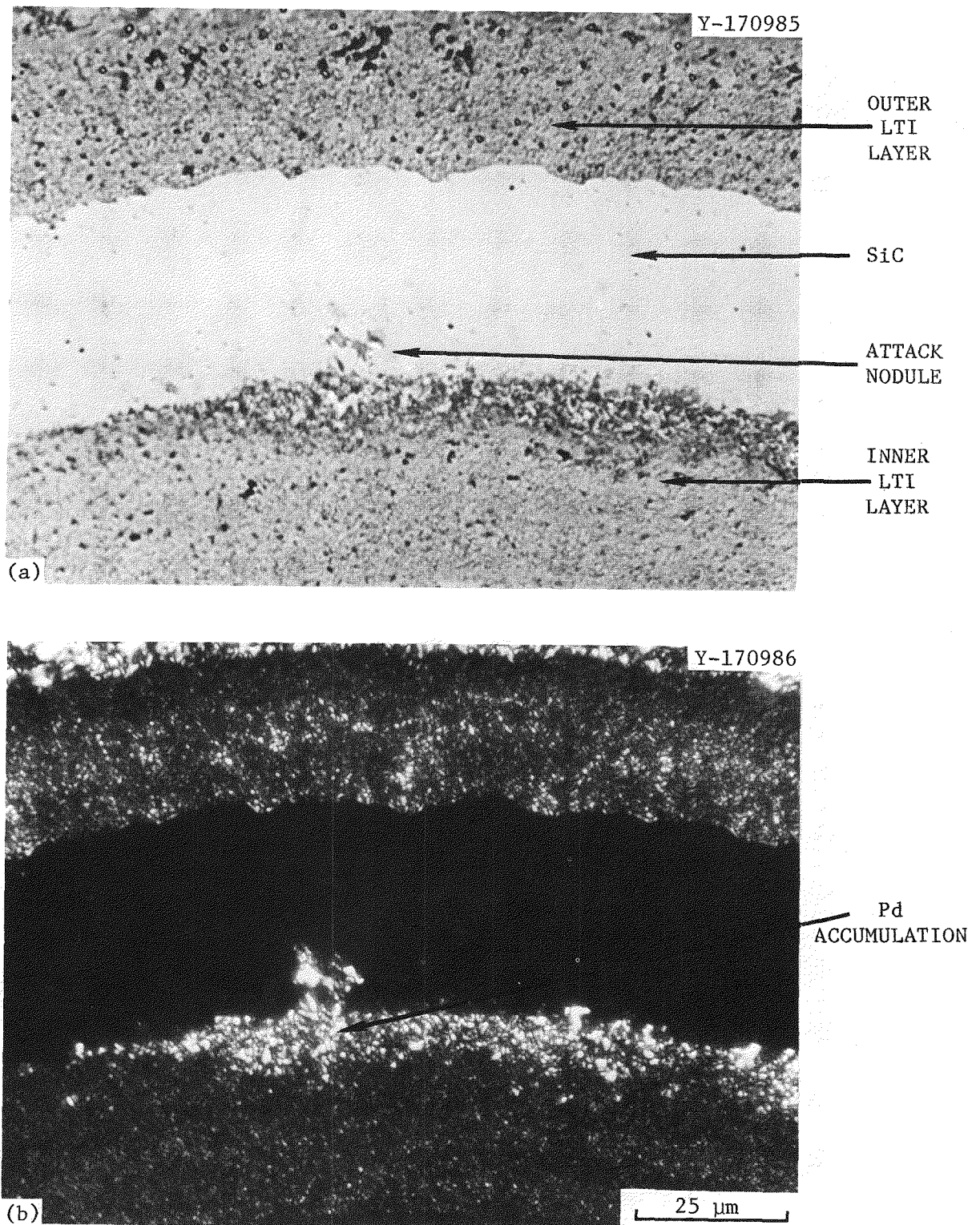
Fig. 6. Site of Pd Attack of SiC After Thermal Gradient Anneal.
(a) Bright field. (b) Polarized light.
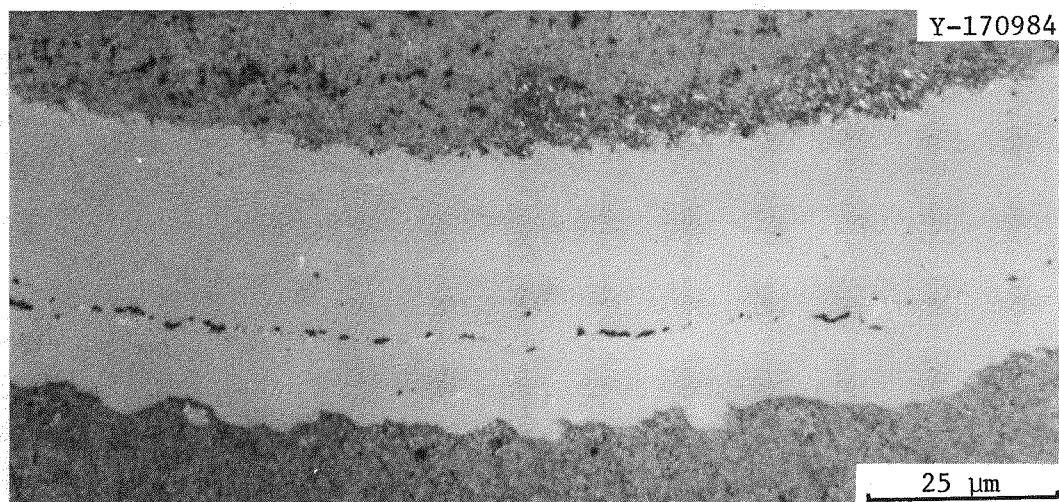
Fig. 7. Metallic Specks (White Spots) Distributed Along Circumferential Striations in a SiC Coating Deposited at 1550°C. These spots are believed to be Pd.

radiograph (to determine its exact temperature during the anneal). Depth of penetration into the SiC was measured to ±0.5 μm, and penetration rate was calculated by dividing by 2000 h. The Appendix lists the results of quantitative metallography. The data were plotted according to the Arrhenius relation

$$P = A \exp(-Q/RT) \; ,$$

where

P = rate of penetration into SiC;

A = preexponential constant;

Q = activation energy for the rate-controlling process;

R = gas constant, 8.314 J/mol K;

T = absolute temperature.

Figure 8 shows the data points from this study and, for comparison, the best fit line from irradiation studies[5] given by A = 46.2 μm/h and Q = 1.358 × 10^5 J/mol. Taking the data from this study only, the activation energy is calculated to be Q_{Pd} = 0.950 × 10^5 J/mol.

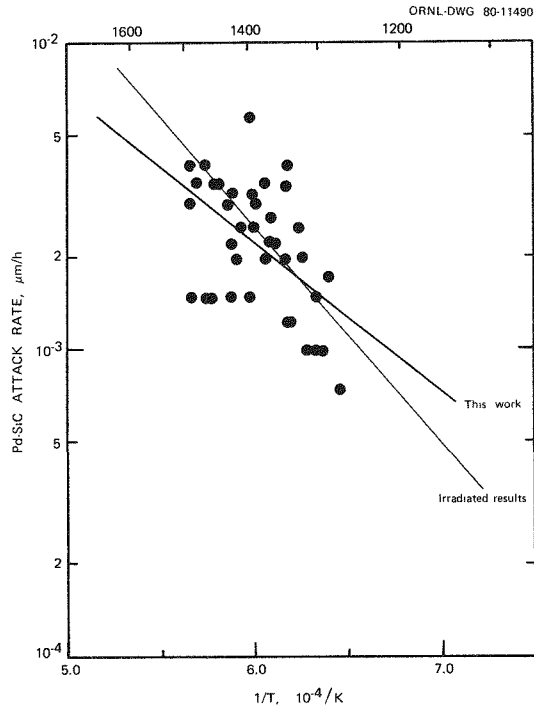Fig. 8. Arrhenius Plot of Attack Rate of SiC by the Fission Product
Element Pd. The activation energy obtained from the slope of the "best
fit" line (using a linear regression) is about 95 kJ/mol. The line
obtained from irradiation experiments passes through these data also.

Considering the experimental uncertainty,[*] the agreement with irra-
diation results is quite good. It should be noted that irradiation data
have a temperature uncertainty of about ±100°C for each particle. For
out-of-reactor data the error is only about ±10°C.

The best fit line from irradiation data passes directly through the
cluster of points from this work, indicating that if the attack is dif-
fusion controlled, it probably results from grain boundary diffusion. The
reason for this is illustrated schematically in Fig. 9. An Arrhenius plot
for diffusion in a polycrystalline material often exhibits a change of
slope, which is interpreted as a change of mechanism from vacancy dif-
fusion to grain boundary diffusion. During irradiation the vacancy con-
centration at low to moderate temperatures is substantially greater than

_____

[*]The accurate measurement of penetration requires that the plane of
polish intersect an attack site close to its maximum depth (an unrealistic
expectation). Thus, the measured value is *at most* the true value and
generally less. Consequently, the highest values are probably more
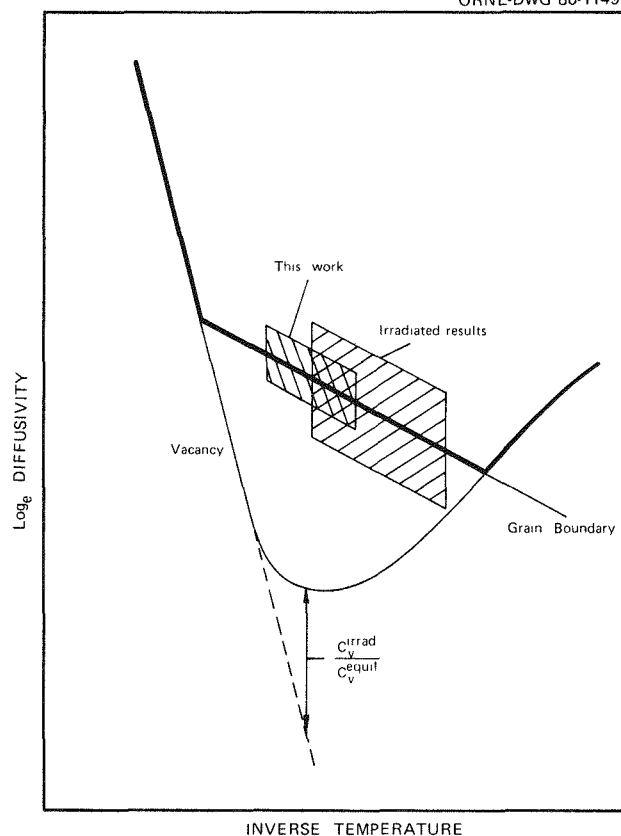accurate.

ORNL-DWG 80-11491

Fig. 9. Schematic Arrhenius Plot for Diffusion in a Polycrystalline Material, Showing that Irradiation Causes Enhanced Vacancy Diffusion at Lower Temperatures. In principle, grain boundary diffusion is not affected. The dominant process at any temperature is that for which the diffusivity is highest (indicated by bold curve). The presumed locations of annealing experiments and irradiations are indicated. The ratio of vacancy concentration during irradiation (C_V^{irrad}) to the equilibrium value (C_V^{equil}) is strongly temperature dependent, as shown.

the equilibrium value, while the activation energy for vacancy motion is essentially constant. Thus, the vacancy contribution to the Arrhenius curve is displaced upward and can increase low-temperature diffusivities by several orders of magnitude.[6] In principle, the grain boundary "leg" is unaffected by irradiation. If vacancy diffusion were dominant in the temperature range of interest here, one would expect the irradiation data to be shifted very noticeably upward relative to the out-of-reactor data. Since that did not occur, it is probable that grain boundary diffusion is the dominant mechanism of Pd attack and transport into the SiC layer. It should also be noted that the activation energy for tracer diffusion of Si in α-SiC has been determined[7] and is about 6 to 7 times greater than the

activation energy determined here for Pd attack. And since Pd is larger than Si, the activation energy for its motion through the SiC lattice is probably yet greater. (The difference in activation energy for diffusion in β- vs α-SiC is not known but is probably small compared with the factor of 6 or 7 noted above.)

The apparent accumulation of Pd in coating striations is particularly interesting. Recent transmission electron microscopic (TEM) studies[2] have shown the striations to consist of bands of porosity separated by bands of small equiaxed grains. Structurally, this must be considered a coating defect. However, it may have a beneficial aspect if it delays release of noble metals by giving them a place to collect. In this sense the striations might be analogous to the buffer PyC layer. We are planning TEM studies to examine some of these coatings after exposure, to determine the phases present in the attack nodules and in the striations, and to further clarify the role of grain boundaries for Pd transport.

The effect of deposition variables on rates of Pd attack is weak. Figure 10 shows the Pd attack rates for all 12 coating batches as a

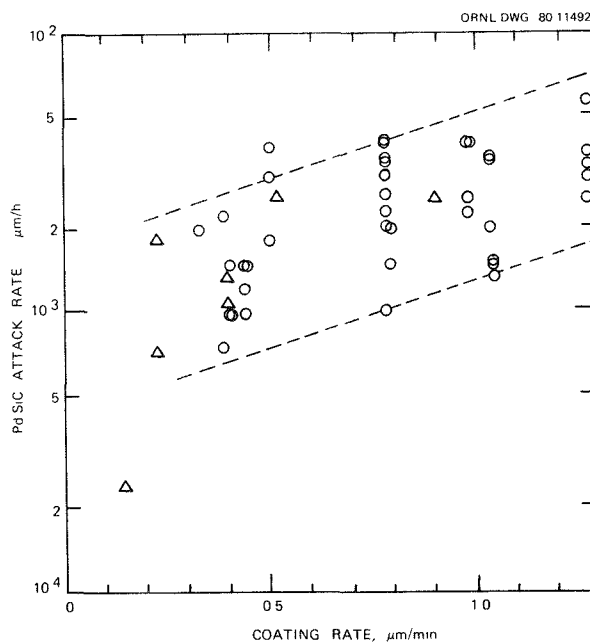Fig. 10. Palladium Attack Rate as a Function of SiC Coating Rate. Triangle points indicate results of irradiation experiments. [Source of irradiation data: T. N. Tiegs, *Fission Product Pd-SiC Interaction in Irradiated Coated Fuel Particles*, ORNL/TM-7203 (April 1980). Note that a typographical error in this source indicated coating rate in micrometers per hour. Micrometers per minute is the correct unit in both studies.]

function of coating rate. Comparisons are difficult since the individual particle temperatures vary somewhat and not enough data exist to select a narrow temperature range for comparison. Nonetheless, the data indicate an increase in Pd attack rate with increasing coating rate. This relationship was also suggested by irradition results, which are included in the figure for comparison.

The correlation between attack rates and deposition temperature is even less obvious and changes form depending on the annealing temperature selected for comparison. This indicates that more data are needed, and for that reason the plots are not presented here.

The relation between Pd attack rates and small-angle x-ray scattering (SAXS) measurements is just now being investigated and will be included in a future report. It has been suggested[8] that coatings with low SAXS intensity might be more resistant to noble-metal attack.

Urania Kernels Containing Silver

In general, the Ag-doped particles exhibited damage to the SiC layer after annealing. The three modes of interaction seen in Pd-doped particles were also observed in Ag-doped specimens. As a rule there was greater penetration by Ag than by Pd. This probably results from the following causes:

1. Silver melts at 960°C, and thus at 1300 to 1500°C one would expect considerable Ag vapor pressure and increased mobility. On the other hand, Pd was not even at its melting point (1550°C) in the temperature range used in this experiment.

2. The Ag-doped particles contained more free metal than did the Pd-doped particles. This made individual attack sites larger and more readily observed.

Figure 11 shows the data for Ag penetration into the SiC layer. The apparent activation energy for this process is $Q_{Ag} = 1.16 \times 10^5$ J/mol. In Fig. 11 the "best fit" line from the Pd data is shown for comparison. Since the activation energies are nearly equal, it is probable that Ag attack is also controlled by diffusion along grain boundaries (or perhaps some other interface).
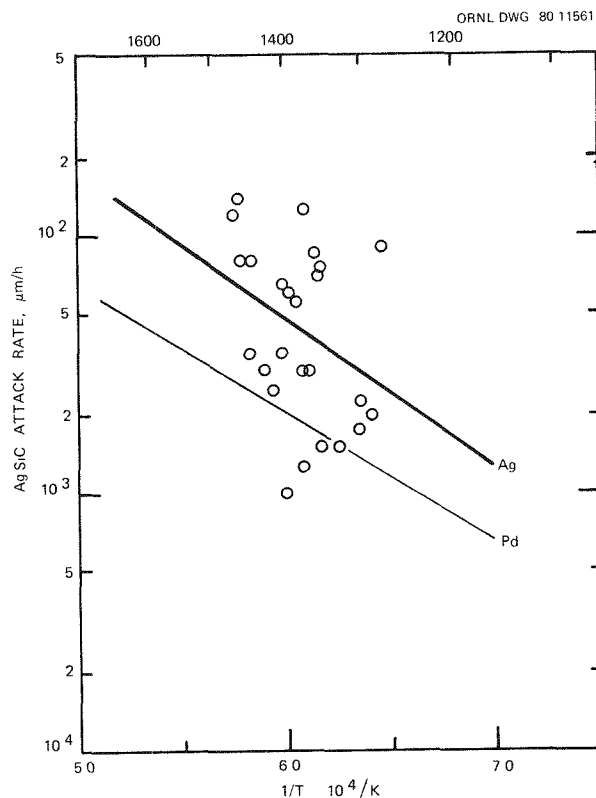
Fig. 11. Arrhenius Plot for the Attack of SiC by Ag. The best fit line for Pd attack is shown for comparison. The activation energy for Ag attack is 116 kJ/mol.

Transmission electron microscopy and electron microprobe analyses will be used to attempt to identify critical diffusion paths for Ag in the SiC layer as well as to study the role of microscopic voids in the coatings. Further optical metallography will be done to increase the data base and, it is hoped, to decrease the scatter present. At that time the effects of coating process variables will be investigated along with the relationship between SAXS intensity and Ag retention. The results of quantitative metallography on Ag-doped particles are given in the Appendix.

CONCLUSIONS

1. Noble-metal attack can be simulated and studied quantitatively by thermal gradient annealing of particles doped with fission product elements, provided the temperatures used are reasonably close to those expected during reactor operation.

2. The fission product elements Ag and Pd attack the SiC layer on HTGR fuel particles. Three modes of interaction are observed: localized attack in small "nodules," specks of free metal surrounded by intact SiC, and free metal accumulations in the circumferential striations present in some coatings.

3. The Pd and Ag appear to be collecting in coating striations (defects in the deposition process). These striations may therefore have a beneficial effect in reducing or halting Pd or Ag migration through the SiC layer.

4. The rate of attack of SiC by Pd observed in out-of-reactor annealing studies is in general agreement with the results of irradiation experiments. The rate of penetration by Ag appears to be more rapid than attack by Pd, but both processes have about the same activation energy.

5. The rate of SiC attack by Ag or Pd at no greater than 1500°C appears to be controlled by diffusion along grain boundaries or some other enhanced-mobility path. For this reason attack rates derived from very high temperature measurements (where vacancy diffusion predominates) cannot safely be extrapolated to pertinent irradiation temperatures.

6. The rate of Pd attack increases with increasing exposure temperature. Higher SiC coating rates cause a slight increase in attack rate, while deposition temperature appears to have little effect.

7. More data are needed, particularly for Ag attack rates. This will increase confidence in the data and possibly allow the effects of deposition variables to be more accurately determined.

manuscript. B. G. Ashdown edited the report, and final report preparation was done by P. T. Thornton of the Metals and Ceramics Division Reports Office.

REFERENCES

1. T. D. Gulden and H. Nickel, "Preface, Coated Particle Fuels," *Nucl. Technol.* 35: 206–13 (September 1977).

2. R. J. Lauf and D. N. Braski, *Dependence of SiC Coating Properties on Deposition Parameters — Preliminary Report*, ORNL/TM-7209 (April 1980).

3. R. J. Lauf, D. N. Braski, and V. J. Tennery, *Characterization of SiC Coatings on HTGR Fuel Particles: Preliminary Report*, ORNL/TM-6940 (August 1979).

4. T. B. Lindemer and R. L. Pearson, "Kernel Migration for HTGR Fuels from the System Th-U-Pu-C-O-N," *J. Am. Ceram. Soc.* 60(1–2): 5–14 (1977).

5. T. N. Tiegs, *Fission Product Pd-SiC Interaction in Irradiated Coated Particle Fuels*, ORNL/TM-7203 (April 1980).

6. P. W. Levy, "Physical Properties of Irradiated Ceramic Materials," pp. 27–32 in *Nuclear Science and Technology for Ceramists, Proceedings of a Symposium, April 7–12, 1966*, National Bureau of Standards, Washington, D.C., May 1967.

7. J. D. Hong, "Self-Diffusion of Carbon-14 and Silicon-30 in Alpha Silicon Carbide Single Crystals," Ph.D. Thesis, N.C. State University at Raleigh, 1978.

8. P. Krautwasser and E. Wallura, "SiC Coating Characterization by Small Angle X-ray Scattering," paper presented at ANS Winter Meeting, San Francisco, Nov. 11–15, 1979.

APPENDIX

Table A1. Quantitative Metallography Results
for UO_2 + Pd Coated Particles

Batch	Particle	Temperature (°C)	Attack Rate (μm/h)
Pd-1	2	1335	1.25
	3	1305	1.50
	1	1460	1.50
	4	1300	1.00
Pd-2	6	1425	2.25
	21	1275	0.75
Pd-3	3	1305	1.00
	1	1470	1.50
	2	1310	1.00
Pd-4	4	1350	2.00
Pd-5	1	1490	1.50
	11	1375	2.00
Pd-6	5	1420	2.00
	11	1360	2.25
	18	1320	1.00
Pd-7	2	1430	3.00
	6	1365	2.75
	14	1290	1.75
Pd-8	1	1480	3.50
	2	1490	4.00
	3	1490	3.00
	5	1465	4.00
	9	1425	3.25
	17	1330	2.50
Pd-9	3	1425	3.25
	4	1400	1.50
	10	1340	1.25
Pd-10	2	1450	3.50
	10	1375	3.50
	13	1325	2.00
Pd-11	4	1390	2.50
	7	1370	2.25
	8	1345	4.00
Pd-12	1	1395	3.25
	2	1390	3.00
	3	1395	5.75
	8	1345	3.50

Table A2. Quantitative Metallography Results
for UO_2 + Ag Coated Particles

Batch	Particle	Temperature (°C)	Attack Rate (μm/h)
Ag-1	3	1455	8.00
	18	1290	2.00
Ag-2	5	1395	6.50
	7	1400	3.50
	8	1370	3.00
	10	1370	1.25
Ag-3	3	1423	3.00
	5	1380	5.50
	15	1300	1.75
Ag-4	4	1390	1.00
	11	1300	2.25
Ag-5	4	1445	8.00
	9	1390	6.00
	11	1350	7.50
	12	1355	8.50
Ag-6	4	1445	3.50
	6	1410	2.50
	12	1350	1.50
Ag-7	12	1370	12.50
Ag-9	7	1365	3.00
	8	1340	1.50
Ag-10	1	1465	12.00
	3	1460	14.00
Ag-11	9	1355	7.00
Ag-12	6	1275	9.00

ORNL/TM-7393
Distribution
Category UC-77

INTERNAL DISTRIBUTION

1–2.	Central Research Library	40.	B. C. Leslie
3.	Document Reference Section	41.	J. S. Lin
4–5.	Laboratory Records Department	42.	E. L. Long, Jr.
6.	Laboratory Records, ORNL RC	43.	M. F. Osborne
7.	ORNL Patent Section	44.	A. E. Pasto
8.	P. Angelini	45.	R. L. Pearson
9.	R. L. Beatty	46.	P. L. Rittenhouse
10.	E. E. Bloom	47.	D. P. Stinton
11.	T. J. Burns	48.	T. N. Tiegs
12.	R. G. Donnelly	49.	A. L. Bement, Jr. (Consultant)
13.	J. I. Federer	50.	E. H. Kottcamp, Jr. (Consultant)
14–16.	M. R. Hill	51.	Alan Lawley (Consultant)
17.	F. J. Homan	52.	T. B. Massalski (Consultant)
18.	M. J. Kania	53.	M. J. Mayfield (Consultant)
19–28.	P. R. Kasten	54.	R. H. Redwine (Consultant)
29.	W. J. Lackey, Jr.	55.	J. T. Stringer (Consultant)
30–39.	R. J. Lauf		

EXTERNAL DISTRIBUTION

56–57. DOE, DIVISION OF NUCLEAR POWER DEVELOPMENT, Washington, DC 20545

Director
G. A. Newby

58. SAN-DEVELOPMENT, SAN DIEGO AREA OFFICE, P.O. Box 81325, San Diego, CA 92138

Senior Program Coordinator

59. DOE, SAN FRANCISCO OPERATIONS OFFICE, 1333 Broadway, Wells Fargo Building, Oakland, CA 94612

Manager

60–61. DOE, OAK RIDGE OPERATIONS OFFICE, P.O. Box E, Oak Ridge, TN 37830

Office of Assistant Manager for Energy Research and Development
Director, Nuclear Research and Development Division

62–227. DOE, TECHNICAL INFORMATION CENTER, P.O. Box 62, Oak Ridge, TN 37830

For distribution as shown in TID-4500 Distribution Category, UC-77 (Gas Cooled Reactor Technology)